Psychiatry Research: Neuroimaging 337 (2024) 111763

Contents lists available at ScienceDirect

Psychiatry Research: Neuroimaging

journal homepage: www.elsevier.com/locate/psychresns

Hyperconnecitivity between dorsal attention and frontoparietal networks predicts treatment response in obsessive-compulsive disorder

Hasan Bakay [a,1,*], Cigdem Ulasoglu-Yildiz [b,c], Elif Kurt [b,c], Tamer Demiralp [b,d], Raşit Tükel [a]

[a] Department of Psychiatry, Istanbul Faculty of Medicine, Istanbul University, Istanbul, Turkey
[b] Hulusi Behçet Life Sciences Research Laboratory, Istanbul University, Istanbul, Turkey
[c] Department of Neuroscience, Aziz Sancar Institute of Experimental Medicine, Istanbul University, Istanbul, Turkey
[d] Department of Physiology, Istanbul Faculty of Medicine, Istanbul University, Istanbul, Turkey

ARTICLE INFO

Keywords:
Resting state functional connectivity
Obsessive-compulsive disorder
Dorsal attention network
Default mode network
Salience network
Frontoparietal network
Treatment effect

ABSTRACT

Obsessive-compulsive disorder (OCD) presented with repetitive obsessions and/or compulsions were associated with disrupted resting-state functional connectivity (rs-FC). To investigate the pharmacological treatment effect on rs-FC changes in OCD patients we conducted the seed-to-voxel FC analyses using dorsal attention network (DAN), default mode network (DMN), salience network (SN) and frontoparietal network (FPN) and basal ganglia seeds. Twenty-two healthy subjects and twenty-four unmedicated OCD patients underwent resting-state functional magnetic resonance imaging. Patients were rescanned after 12 weeks of escitalopram treatment. We found increased FC both within the DAN and between the DAN and the FPN which was ameliorated after medication and correlated significantly with the clinical improvement in obsession scores. We also observed an anti-correlation between the left caudate and the supplementary motor area in unmedicated OCD patients which also normalized with treatment. Results further showed treatment related normalization of orbitofrontal cortex hyperconnectivity with DMN and hypoconnectivity with DAN whereas aberrant FC between the SN and visual areas appears to be a medication effect. We suggest that DAN to FPN hyperconnectivity which is positively correlated with clinical improvement in obsession scores at pre-treatment stage in present study has a potential for being a neuroimaging marker to predict the treatment response in OCD.

1. Introduction

Obsessive-compulsive disorder (OCD) is a generally chronic disease that can significantly affect the functionality of the person, with repetitive obsessions and/or compulsions (Abramowitz et al., 2009). Studies about brain regions associated with OCD have been conducted with various neuroimaging methods, especially the fMRI, which provides the opportunity to examine the functional connectivity and task-related activity changes. Numerous functional neuroimaging studies have revealed that dysfunction in the frontal subcortical circuits plays a role in the pathogenesis of OCD (Saxena et al., 1998; Hou et al., 2012, 2014). The orbito-fronto-subcortical circuit proposed by Saxena et al. (1998) has been accepted as a basic model in the neurobiology of OCD. In this model, the existence of an orbitofrontal loop consisting of projections starting from the orbitofrontal cortex (OFC) to the caudate nucleus and ventral striatum, then to the dorsomedial thalamus via internal pallidus and back to the OFC from the thalamus was asserted. Subsequent research has claimed that the underlying pathology of the disease is not limited to orbitofronto-striatal regions and associated limbic structures, but also involves abnormalities in additional brain areas, particularly more lateral frontal and parietal regions which may be considered as dorsolateral prefronto-striatal circuit (Menzies et al., 2008). Additionally, many fMRI studies have reported activity changes in the OFC, anterior cingulate cortex (ACC), subcortical areas (Hou et al., 2012; Fan et al., 2017; Ping et al., 2013) and also temporal cortex (Yang et al., 2019), parietal cortex (Xu et al., 2019) and occipital cortex (Chen et al., 2016; Tian et al., 2016).

Many studies using resting-state data exhibited abnormal functional connectivity within and between the default mode network (DMN), salience network (SN), and frontoparietal network (FPN) (Stern et al., 2012; Chen et al., 2018; Fan et al., 2017). Gürsel et al. (2018) conducted a meta-analysis of resting-state networks in OCD, in which impaired

* Corresponding author.
E-mail address: hasanbakay@gmail.com (H. Bakay).
[1] Present address: Department of Psychiatry, Meram Faculty of Medicine, Necmettin Erbakan University, Konya, Turkey.

https://doi.org/10.1016/j.pscychresns.2023.111763
Received 10 April 2023; Received in revised form 31 October 2023; Accepted 21 November 2023
Available online 23 November 2023
0925-4927/© 2023 Elsevier B.V. All rights reserved.

connectivity between the DMN, SN and FPN was reported. DMN is involved in reflective and introspective self-referring processes, while FPN plays a crucial role in action planning and response inhibition. SN is associated with regulating external and internal salient information (Cui et al., 2020). Abnormal functional connectivity both within and between the FPN, SN and DMN, which is named the "triple network" model (Menon, 2011), provides important insight about the pathophysiology of OCD (Gürsel et al., 2018). In this model, the SN is involved in both filtering and detecting the salient information interfering with the FPN and DMN functions. In other words, SN plays an important role in switching the activities of the DMN (Chen et al., 2018) and FPN (Gürsel et al., 2020).

Selective serotonin reuptake inhibitors (SSRIs) and cognitive-behavioral therapy (CBT) are the first-line treatment options for OCD. Few functional neuroimaging studies on the potential neurobiological mechanisms and predictors of response to CBT in OCD have provided results associated with either fronto-striatal circuitry or with ICNs (Yang et al., 2015; Moody et al., 2017; Li et al., 2018; Reggente et al., 2018). Yang et al. (2015) showed decreased regional homogeneity (ReHo) in the bilateral middle frontal cortex, right OFC, and increased ReHo in the left caudate along with the clinical improvement after CBT. Li et al. (2018) reported that CBT normalized the aberrant resting-state functional connectivity (rs-FC) between the right OFC and left dorsolateral prefrontal cortex. Reggente et al. (2018) showed that rs-FC within the DMN and visual network predicted OCD symptom severity after CBT.

Similarly, neuroimaging studies on the SSRI effects in OCD have reported either regulation of the increased connectivity in the orbito-fronto-striatal circuit by antidepressant medication through the reduction of the local ventral striatal connectivity (Beucke et al., 2013), or treatment-related changes in large-scale connectivity networks (Shin et al., 2014b). The authors reported reduced small-world efficiency and functional association between the DMN and FPN in OCD, while the elevation of the small-world efficiency, modular organization, and connectivity degree accompanied clinical improvement after 16 weeks of SSRI treatment.

Although there is a growing literature focusing on the "triple network" model in the pathogenesis of OCD, current literature indicates that other networks are also in play. For example, the dorsal attention network (DAN), used as seed only in a few resting-state fMRI (rs-fMRI) studies, draws attention by showing aberrant connectivity in OCD (Brennan et al., 2019).

Our study, adding the large-scale ICNs to the conventional fronto-striatal circuitry, investigated rs-FC changes in adult OCD patients and the effects of medication (escitalopram) on them with a seed-based approach, where the seed regions include basal ganglia as core structures of the fronto-striatal circuit as well as the main nodes of the FPN, DMN and SN of the triple network model. Additionally, main nodes of the DAN, recently shown to be associated with the obsession severity (Lee et al., 2020), were also included in the analyses. By computing the seed-to-voxel connectivities between these regions and all brain voxels, we assume that a comprehensive view of the pathophysiological changes within and between the related circuits or networks can be obtained. Strict inclusion criteria, recruitment of unmedicated patients with no comorbidity and detailed comparison of the pre- and post-treatment findings further helped in obtaining a more complete view of the neurobiology and pathogenesis of OCD.

2. Methods

2.1. Participants

24 unmedicated OCD patients without any psychiatric comorbidity and 22 healthy controls (HCs) with similar mean age, education level and gender distribution participated in the study. One OCD patient and two HCs were excluded from the study due to poor data quality. Additionally, two patients couldn't participate in the second fMRI session after three months pharmacological treatment and were excluded from the study. Hence, the final cohort for rs-fMRI analyses consisted of 21 OCD patients and 20 HCs.

All subjects gave their informed consent before participating in the study. The local ethics panel of the Istanbul University, Istanbul Faculty of Medicine approved the study (IRB20141946).

Inclusion criteria for OCD group were, (1) being diagnosed with OCD by Structured Clinical Interview for DSM-IV/Clinical Version (SCID-I/CV), (2) having Yale-Brown Obsessive-Compulsive Scale (Y-BOCS) total score of 16 or higher, (3) aged between 18 and 50, (4) taking no psychotropic medication for the last 6 weeks (8 weeks for fluoxetine). Exclusion criteria for OCD group were, (1) diagnosis of another psychiatric disorder from OCD with SCID-I/CV and (2) having a history of another medical disease. Exclusion criteria for HC group were, (1) being diagnosed with any psychiatric disorder according to DSM-IV criteria, (2) using any psychotropic medication, (3) presence of any psychiatric disorder in first-degree relatives. Other exclusion criteria for both groups were, (1) having an acute or chronic physical disease, (2) presence of a neurological disorder such as seizure, central nervous system infection, cerebrovascular disease, head trauma history requiring more than 30 min of unconsciousness or hospitalization, (3) having a history of alcohol or substance abuse / addiction and (4) pregnancy or lactation.

2.2. Clinical assessment

All patients underwent the Hamilton Anxiety Rating Scale (HAM-A), Hamilton Depression Rating Scale (HAM-D), Quality of Life Enjoyment and Satisfaction Questionnaire (Q-LES-Q), SCID-I/CV, Clinical Global Impression Scale (CGI), Sheehan Disability Scale (SDS), Y-BOCS and Overvalued Ideas Scale (OVIS). These scales have been applied before and after three months pharmacological treatment. HAM-A, HAM-D and Q-LES-Q have also been applied to the HCs.

2.3. Pharmacological treatment

The patient group (9 were medication-naïve) consisted of OCD patients who were unmedicated for at least 6 weeks (8 weeks for fluoxetine). All of the patients reported that they had not received cognitive behavioral therapy or psychodynamic psychotherapy before. After the clinical scales were applied, fMRI recordings were obtained, and escitalopram 10 mg/day was prescribed to the patients. Clinical interviews were conducted with patients at the second and sixth weeks of their treatment to closely monitor and encourage adherence to treatment. Escitalopram treatment was increased to 20 mg/day in the second week of the treatment and to 30 mg/day in the sixth week of treatment. Clinical scales and fMRI scans were reapplied at the 12th week of treatment.

2.4. MRI data acquisition

All MRI scans were acquired on a 3T scanner (Philips Achieva, Philips Medical Systems, The Netherlands) equipped with a SENSE 32 channel head coil. High-resolution 3D T1-weighted MR images were collected using a Turbo Field Echo (TFE) sequence with 250 × 250 mm field of view (FOV), 160 axial slices, 1 mm slice thickness (without gap), TR/TE=7.7/3.8 ms, acquisition matrix 252 × 209. rs-fMRI data were obtained using an EPI sequence with the repetition time (TR)=2000 ms, echo time (TE)=30 ms, flip angle=90°, FOV=224 × 240 mm, acquisition matrix size=112 × 117, voxel size=2 × 2 × 4 mm^3 in-plane resolution. Following 10 dummy volumes, 212 vol were acquired each containing 36 axial slices to cover the whole brain. During rs-fMRI, all participants were instructed to remain awake and lie in a relaxed position with closed eyes, and not focus on anything in particular.

2.5. MRI data preprocessing

The MRI data preprocessing was performed using Statistical Parametric Mapping version 12 (http://www.fil.ion.ucl.ac.uk/spm/) preprocessing steps as included in the CONN functional connectivity toolbox version 18.b (https://www.nitrc.org/projects/conn) (Whitfield-Gabrieli and Nieto-Castanon 2012). First, in order to adjust the head motions, functional images were realigned to the first image. Minimum movement and rotation thresholds to be included in the analyses were determined as less than ±3 mm translation in the x, y, or z directions and less than ±3° rotation in each axis respectively. One healthy subject and one OCD patient were excluded from the rs-fMRI analyses due to larger head motions. Additionally, the artifact detection tool was used for the identification of outlier scans for scrubbing. The global-signal z-value threshold for signal intensity outliers was set at 5 standard deviations greater than or less than the mean and the threshold value for difference in composite motion was set as 0.9 mm. One healthy subject with outlier volumes more than 20 % (>43) of the total number of functional volumes (212) was excluded from further analysis. Afterwards, functional and structural data were coregistered. The anatomic data was segmented into white matter (WM), gray matter (GM), and cerebrospinal fluid (CSF), and normalized to the Montreal Neurological Institute (MNI) standard space. Subsequently, spatial normalization into MNI space was carried out for the realigned functional images using the resulting transformation matrix and resampling of the data to 2 mm^3 voxels. Finally, spatial smoothing was applied to the normalized functional images using an 8 mm full width half maximum Gaussian kernel.

2.6. Functional connectivity analyses

Seed to voxel functional connectivity analyses were performed using the CONN toolbox (Whitfield-Gabrieli and Nieto-Castanon 2012). During the denoising step, we utilized the default CONN preprocessing pipeline to eliminate undesirable motion, physiological, and other artifactual effects from the BOLD signal before calculating connectivity measures (Nieto-Castanon, 2020). The CONN toolbox applies the component-based noise correction method (CompCor), which uses the participant-specific eroded WM and CSF anatomic masks and applies principal component analysis (PCA) on the BOLD signals of the voxels within these masks in order to estimate the nuisance confounds (Chai et al., 2012). These nuisance confounds included 5 components from the WM and 5 components from the CSF. Additionally, 12 estimated participant-motion parameters (6 parameters from realignment and their first-order temporal derivatives), participant-specific outlier scans (identified through scrubbing), and the effect of session and its first-order derivative convolved with the canonical hemodynamic response function were regressed out from the data, while we preferred not to implement a global signal regression. Finally, linear detrending and temporal band-pass filtering (0.01–0.1 Hz) was applied on each run individually prior to functional connectivity analyses.

A total of 19 seeds were used for functional connectivity analyses. The CONN toolbox offers a set of 32 HCP-ICA network seeds derived from the ICA analysis on the Human Connectome Project (HCP) dataset (Nieto-Castanon and Whitfield-Gabrieli, 2020). 15 seeds corresponding to the major nodes of the 4 cognitive networks according to this scheme were included in our analyses: medial prefrontal cortex (MPFC) and posterior cingulate cortex (PCC) seeds for DMN, ACC, left and right anterior insulae (AI) and supramarginal gyri (SMG) for SN, left and right frontal eye fields (FEF) and intraparietal sulci (IPS) for DAN and left and right lateral prefrontal cortices (LPFC) and posterior parietal cortices (PPC) for FPN. Important nodes of the basal ganglia network corresponding to left and right caudate and putamen according to the FSL Harvard-Oxford Atlas were also included in the analyses.

Subject level FC analysis was performed by calculating the bivariate correlation coefficients between the average time courses for each seed with the time courses of all other voxels in the brain. Second level analyses were performed on Fisher's z-transformed correlation coefficients. FC differences at rest were investigated between unmedicated OCD patients and HCs by independent-samples *t*-tests. Secondly, treatment effect was investigated by comparing the pre- and post-medication data of the OCD patients by paired-samples *t*-tests. To elaborate the effect of medication on the FCs, we also compared the medicated OCD and HC groups for the seeds that significantly changed their connectivity patterns between medicated and unmedicated states of the patients. The voxel-based FC results were thresholded using an initial cluster-forming height threshold set at $p<0.001$ (uncorrected) followed by a FWE-corrected $p<0.05$ cluster-level threshold. Significance threshold was also adjusted for multiple comparisons (i.e., number of seeds; $p_{FWE\text{-}corr}<0.0026$; 0.05/19).

2.7. Correlations of the functional connectivities with clinical improvement

The correlation analysis between the clinical scores and the FC findings were limited to those seeds which displayed a significant difference between the unmedicated patients and HCs and showed a change towards normal values after medication. In order to estimate any predictive value of the FC on clinical improvement, the baseline FC values of these specific areas in the pre-treatment group were tested for correlations with the percent change of the Y-BOCS scores due to treatment, which assess the severity of obsessions and compulsions.

For this purpose, percentage of the clinical improvement was calculated as the change in symptom severity after treatment according to baseline obsession and compulsion scores of the Y-BOCS. Using the ROI extraction tool (REX), the baseline (pre-treatment) connectivity values within particular ROIs were extracted for each individual OCD patient. Spearman's correlation coefficients were calculated between the average connectivity values of these ROIs in the pretreatment data and percentage of the clinical improvement. Statistical results were Bonferroni corrected for the number of ROIs and clinical scores tested.

2.8. Clinical data analyses

Statistical analysis was performed using SPSS software (IBM SPSS Statistics for Windows, Version 24.0). For between-group analysis, i.e., HC vs OCD patients at baseline, Mann-Whitney *U* test was used as the data was not normally distributed. For within-group analysis, i.e., the baseline vs follow-up comparisons of the OCD patients, paired sample *t*-test and Wilcoxon signed-ranks test was used for the normal and non-normally distributed data.

3. Results

3.1. Demographics and clinical data

There was no significant difference between two groups in terms of age, years of education and gender (all *p* values > 0.05) (Table 1).

Table 1
Demographics of the participants included in the rs-FC analysis.

	HC ($n = 20$)	OCD ($n = 21$)	*test*	*p*
Age (Mean ± SD, min−max)	26.75 ± 7.39 (18 − 42)	28.48 ± 8.51 (18 − 43)	$t =$ 0.692	0.493
Years of education	12.7 ± 3.4 (5 − 18)	12.67 ± 3.93 (5 − 18)	$t =$ 0.029	0.977
Gender (Female/Male)	13/7	15/6	$\chi^2 =$ 0.658	0.744
Inter-scan-interval (days)	—	93.38 ± 13.19 (84 − 141)	—	—

HC: healthy control, OCD: obsessive-compulsive disorder, SD: standard deviation.

3.2. Treatment response

OCD patients displayed significant clinical improvement compared with their baseline assessments after 12 weeks of treatment (Table 2). Significant reductions in the symptom severity for obsession, compulsion and HAM-A scores were observed at follow-up, with a general improvement in functioning (all p values<0.05) (For details, please see Table 2).

3.3. Functional connectivity findings

Seed-to-voxel FC analyses conducted on the rs-fMRI data with 19 seeds revealed significant differences between the unmedicated OCD patients and HCs for 2 of the seeds which were left FEF of the DAN and left caudate. When we compared the pre- and post-medication OCD patients, treatment effects were obtained for the right IPS of the DAN, the MPFC seed of the DMN, the ACC and right SMG seeds of the SN, in addition to the aforementioned seeds above. The FC maps of these seeds are shown in Fig. 1 separately for the HCs, the unmedicated and medicated OCD patients. Finally, all 6 seeds affected by the medication were compared between medicated OCD patients and the HCs, which revealed no significant FC difference for any of the seeds. The significant results are summarized in Tables 3 and 4.

No statistically significant results were obtained for the PCC, left and right AI, left SMG, right FEF, left IPS, left and right LPFC and PPC, right caudate and left and right putamen seeds, neither between unmedicated OCD patients and healthy controls nor between the pre- and post-medication OCD patients.

3.3.1. Altered functional connectivity of FEF and the effect of treatment

In unmedicated OCD patients, left FEF showed significant connectivity increases with two clusters compared to HCs; the left ($p_{FWE\text{-}corr}$=0.0005) and the right IPL ($p_{FWE\text{-}corr}$=0.0009) (Table 3 and Fig. 2A). The increased connectivity of the left FEF with the right IPL in OCD patients showed a significant reduction after the treatment ($p_{FWE\text{-}corr}$ = 0.000001) (Table 4 and Fig. 2B), while its FC with the left IPL also tended towards the values observed in the HC group, although its reduction relative to the premedication was not significant (Fig. 2A). In any case, final comparison of the medicated OCD patients with HC did not reveal significant differences regarding the connectivity of the left FEF neither with the right nor with the left IPL. The correspondence of the right and left IPL clusters resulting from comparisons between both the HC vs unmedicated OCD groups and unmedicated vs medicated OCD groups were visualized by overlapping these areas with the closely located posterior nodes of the DAN and FPN networks (Fig. 3), which indicated that they overlapped with both networks.

3.3.2. Altered functional connectivity of the left caudate and the effect of treatment

The left caudate's correlations with a cluster corresponding to bilateral supplementary motor areas (SMA) displayed a significant change to negative values in the unmedicated OCD patients compared to HCs ($p_{FWE\text{-}corr}$=0.0025) (Table 3 and Fig. 4A). This difference was not present in the comparison between the medicated OCD patients and HCs, but the treatment introduced a significantly increased anticorrelation with a cluster corresponding to the left superior occipital cortex (SOC) and cuneus ($p_{FWE\text{-}corr}$=0.0007) (Table 4 and Fig. 4B). This medication-related connectivity change introduced no significant difference between the medicated OCD patients and HCs, since the HCs also displayed a weak anticorrelation between the caudate nucleus and these occipital areas.

3.3.3. Effect of treatment on functional connectivity of other seed regions than those affected in unmedicated OCD patients

Although there was no difference for the DMN and SN seeds between unmedicated OCD patients and HCs, the treatment resulted in significant FC changes of the MPFC seed of DMN, the ACC and right SMG seeds of SN, and the right IPS seed of the DAN.

After treatment, MPFC showed a significant hypoconnectivity with two clusters corresponding to the left and right orbitofrontal cortices (OFC) ($p_{FWE\text{-}corr}$=0.00008 and $p_{FWE\text{-}corr}$=0.0013, respectively). Although there was no significant connectivity difference for this seed between unmedicated OCD patients and HCs, the bar graph reflects that this treatment effect is associated with the reduction of the increased connectivity in the OCD patients towards normal values (Fig. 5).

The treatment also introduced a significant hypoconnectivity of the right SMG with a cluster corresponding to the bilateral thalami ($p_{FWE\text{-}corr}$=0.001) (Table 4 and Fig. 6). Similar to the previous treatment result, the right SMG did not reveal any significant connectivity difference between the HCs and unmedicated OCD patients. However, the medication effect in this area seems to stem from a reduction of the increased connectivity between right SMG and thalamus in OCD towards normal values (Fig. 6, bar graph), which is supported by the absence of any connectivity difference between the HC and the medicated OCD patients for these areas.

Another treatment effect was increased right IPS connectivity with the right OFC ($p_{FWE\text{-}corr}$=0.0012) (Table 4, Fig. 7), although not significant in unmedicated OCD patients compared with the HC (Fig. 7, bar graph). The absence of any significant difference for this seed in the HC vs medicated OCD comparison points also to an ameliorating effect of the medication for this connectivity.

Finally, ACC displayed no evident connectivity with the bilateral cunei in neither the HC group nor in the unmedicated OCD patients, but

Table 2
Clinical characteristics of the patients. Comparisons of the scales between HC and unmedicated patients and between medicated and unmedicated patients.

	HC (n = 20) Mean ± SD (min – max)	OCD-premed (n = 21)	OCD-postmed (n = 21)	HC vs OCD-premed *test*	*p*	OCD-postmed vs OCD-premed *test*	*p*
Disease Duration (yrs)	–	5.31 ± 6.48 (0.5 – 30)	–				
HAM-A	3.35 ± 2.18 (0 – 9)	12.76 ± 5.58 (5 – 26)	5.29 ± 3.41 (1 – 15)	U = 11.5	<0.001	Z = 3.984	<0.001
HAM-D	1.9 ± 1.29 (0 – 4)	10.52 ± 5.18 (2 – 19)	3.62 ± 2.09 (0 – 8)	U = 15.5	<0.001	Z = 4.021	<0.001
Q-LES-Q	51.65 ± 3.6 (44 – 57)	40.57 ± 8.03 (23 – 52)	52.81 ± 6.54 (41 – 70)	U = 29	<0.001	Z = 4.017	<0.001
Y-BOCS Obsession	–	14.62 ± 2.13 (10 – 18)	7.57± 3.92 (1 – 16)			t = 9.383	<0.001
Y-BOCS Compulsion	–	14.38 ± 2.29 (10 – 19)	8.48 ± 3.87 (2 – 16)			t = 9.455	<0.001
Y-BOCS Total	–	29 ± 3.56 (23 – 37)	16.05 ± 7.49 (3 – 32)			t = 10.309	<0.001
OVIS	–	3.49 ± 0.87 (2 – 5.4)	2.88 ± 0.74 (1.8 – 4.5)			Z = 3.927	<0.001
SDS Work	–	6 ± 1.97 (3 – 9)	2.86 ± 1.77 (0 – 6)			Z = 3.952	<0.001
SDS Social life	–	6 ± 1.92 (2 – 9)	2.43 ± 1.6 (0 – 5)			Z = 4.055	<0.001
SDS Home	–	5.57 ± 2.16 (0 – 9)	2.57 ± 1.78 (0 – 7)			Z = 3.933	<0.001
CGI Severity	–	4.67 ± 0.58 (4 – 6)	–				
CGI Improvement	–	–	2.24 ± 0.89 (1 – 4)				

CGI: Clinical Global Impression Scale, HAM-A: Hamilton Anxiety Rating Scale, HAM-D: Hamilton Depression Rating Scale, OVIS: Overvalued Ideas Scale, Q-LES-Q: Quality of Life Enjoyment and Satisfaction Questionnaire, SDS: Sheehan Disability Scale, Y-BOCS: The Yale–Brown Obsessive Compulsive Scale. OCD-premed: unmedicated OCD patients, OCD-postmed: OCD patients after treatment, HC: healthy control.

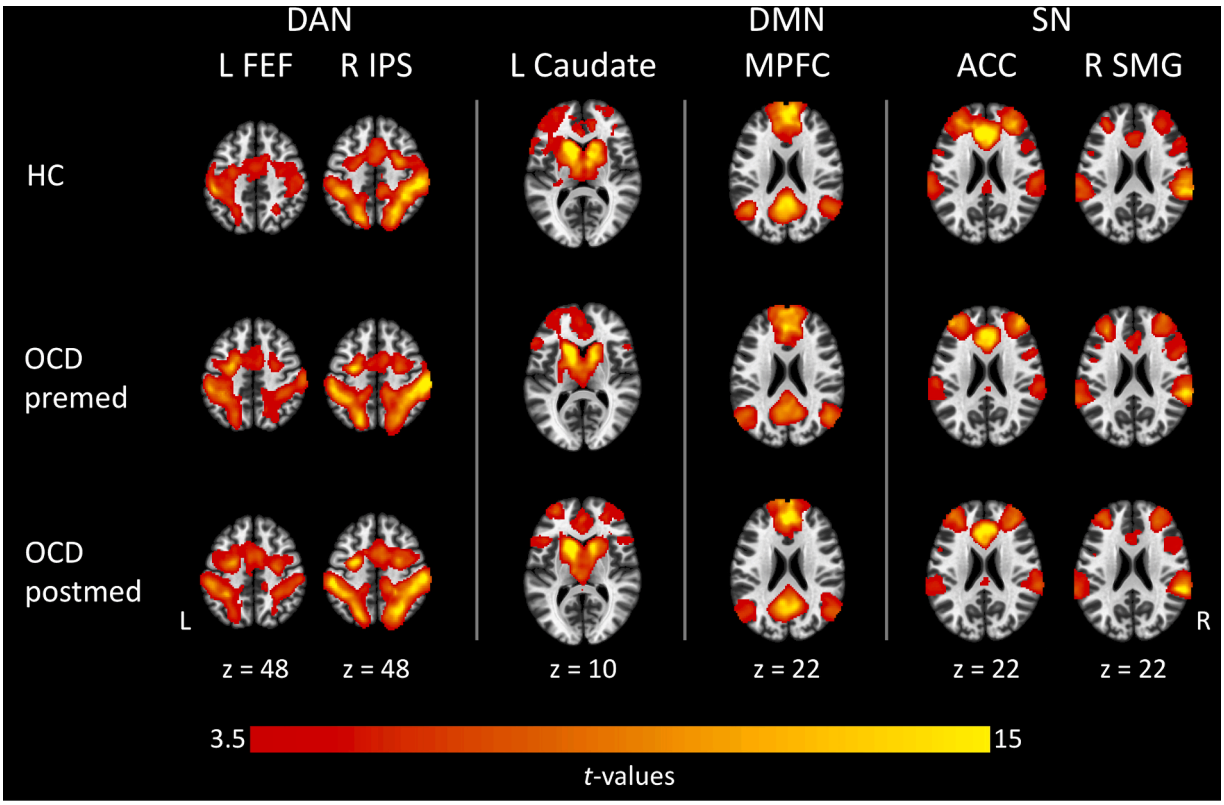


Fig. 1. Functional connectivity maps for the DAN, left caudate, DMN and SN of the HCs, and OCD patients at premedication and postmedication. DAN FC maps obtained separately by using the left FEF and right IPS seeds. DMN FC maps obtained by using the MPFC seed. SN FC maps obtained by using the ACC and right SMG seeds. Typical DAN and SN obtained using MPFC seed and ACC and right SMG seeds are shown.
AAC: anterior cingulate cortex, DAN: dorsal attention network, FPN: frontoparietal network, HC: healthy control, IPS: intraparietal sulcus, MPFC: medial prefrontal cortex, OCD-premed: unmedicated OCD patients, OCD-postmed: OCD patients after treatment, PPC: posterior parietal cortex, SMG: supramarginal gyrus, SN: salience network. L: left, R: right.

Table 3
Seed-to-voxel FC results of comparisons between OCD-premed and HCs (cluster forming threshold of $p<0.001$ uncorrected combined with cluster level threshold $p_{FWE\text{-}corr} < 0.0026$).

Seed Region	Regions showing connectivity changes	Group Contrast	Cluster Size	Peak coordinates (x y z)	T_{max}	$p_{FWE\text{-}corr}$
DAN – L FEF	L IPL	OCD-premed > HC	514	−48 −28 32	5.14	0.0005
	R IPL		474	58 −26 52	4.85	0.0009
L Caudate	Bilateral SMA	OCD-premed < HC*	383	10 −4 58	5.19	0.0025

* indicates increased anticorrelation
DAN: dorsal attention network, FEF: frontal eye field, IPL: inferior parietal lobule, SMA: supplementary motor area, OCD-premed: unmedicated OCD patients, HC: healthy control, L: left, R: right.

Table 4
Seed-to-voxel FC results of comparisons among OCD-premed and OCD-postmed (cluster forming threshold of $p<0.001$ uncorrected combined with cluster level threshold $p_{FWE\text{-}corr} < 0.0026$).

Seed Region	Regions showing connectivity changes	Group Contrast	Cluster Size	Peak coordinates (x y z)	T_{max}	$p_{FWE\text{-}corr}$
DAN – L FEF	R IPL	OCD-postmed < OCD-premed	758	58 −22 54	6.95	0.000001
DAN – R IPS	R OFC	OCD-postmed > OCD-premed	353	50 32 −20	5.48	0.0012
L Caudate	L SOC and Cuneus	OCD-postmed < OCD-premed*	347	−18 −100 22	4.68	0.0007
DMN – MPFC	L OFC	OCD-postmed < OCD-premed	515	−22 42 −20	5.96	0.00008
	R OFC		350	24 46 −22	5.07	0.0013
SN – R SMG	Bilateral thalami	OCD-postmed < OCD-premed	352	−6 −18 −2	6.26	0.001
SN – ACC	Bilateral Cunei	OCD-postmed < OCD-premed*	395	6 −88 28	5.40	0.0005

* indicates increased anticorrelation
ACC: anterior cingulate cortex, DAN: dorsal attention network, DMN: default mode network, FEF: frontal eye field, IPL: inferior parietal lobule, IPS: intraparietal sulcus, MPFC: medial prefrontal cortex, OFC: orbitofrontal cortex, SMG: supramarginal gyrus, SN: salience network, SOC: superior occipital cortex. OCD-premed: unmedicated OCD patients, OCD-postmed: OCD patients after treatment, L: left, R: right.

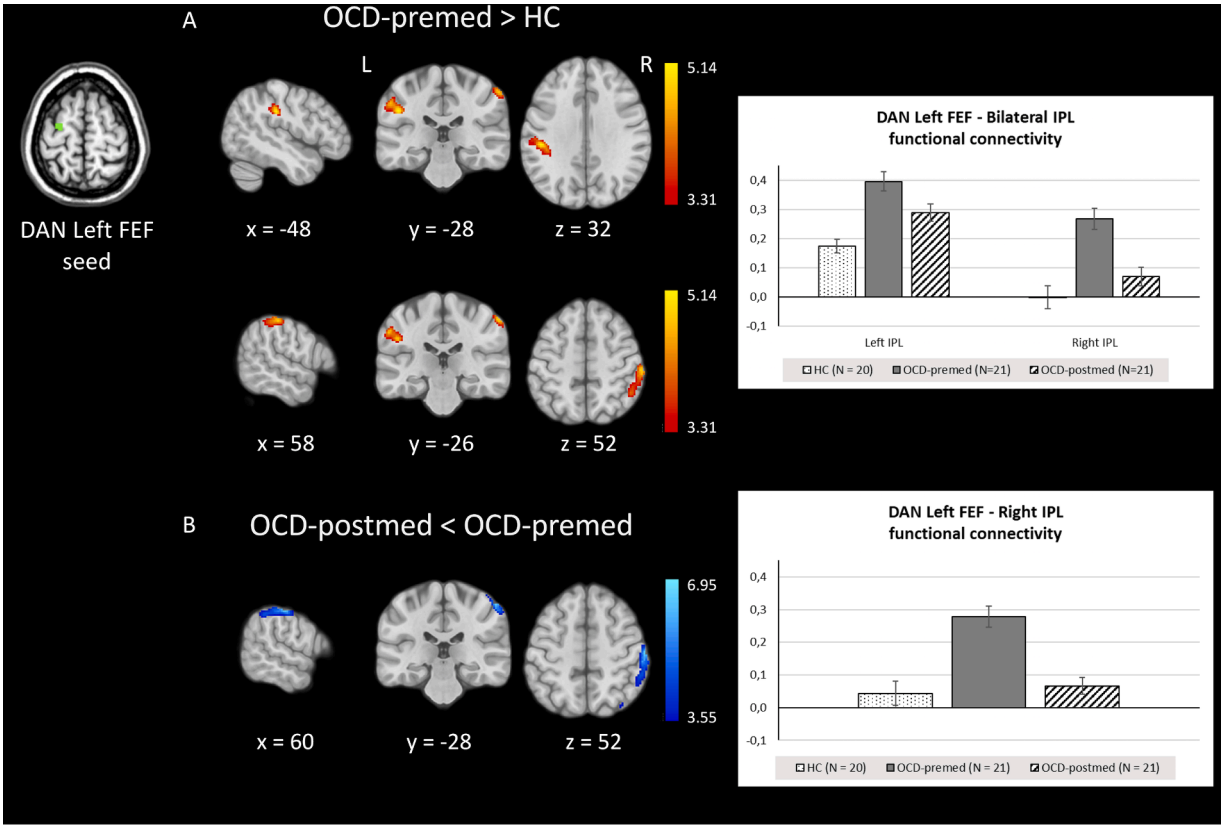


Fig. 2. Functional connectivity differences for the left FEF seed probing the DAN. **A)** Hyperconnectivity with bilateral IPL in OCD-premed compared to HCs. **B)** Hypoconnectivity with right IPL in OCD-postmed compared to OCD-premed (cluster forming threshold uncorrected $p < 0.001$, cluster-level $p_{FWE\text{-}corr} < 0.0026$). Bar graphs depicting the correlation values for HC, OCD-premed and OCD-postmed.
DAN: dorsal attention network, FEF: frontal eye field, OCD-premed: unmedicated OCD patients, OCD-postmed: OCD patients after treatment, HC: healthy control. L: left, R: right.

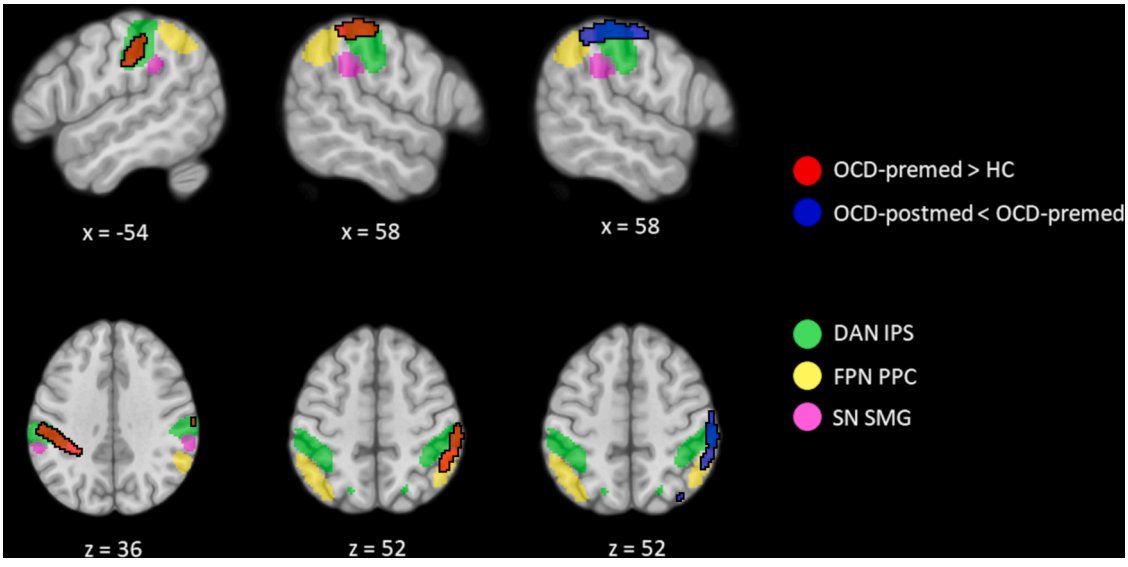


Fig. 3. Right and left IPL regions resulting from the unmedicated OCD > HC (red) and medicated OCD < unmedicated OCD (dark blue) comparisons were superimposed on the sagittal and axial T1-weighted MNI-152 template image. Green, yellow and pink colors indicate the DAN-IPS, FPN-PPC and SN-SMG nodes of the CONN toolbox, respectively. Significant clusters superimposed on these nodes show that they were highly overlapping both with the DAN-IPS and FPN-PPC nodes, but not with the SN-SMG node.
DAN IPS: intraparietal sulcus seed of the dorsal attention network, FPN PPC: posterior parietal cortex seed of the frontoparietal network, HC: healthy control, OCD-premed: unmedicated OCD patients, OCD-postmed: OCD patients after treatment, SN SMG: supramarginal gyrus seed of the salience network, L: left, R: right.

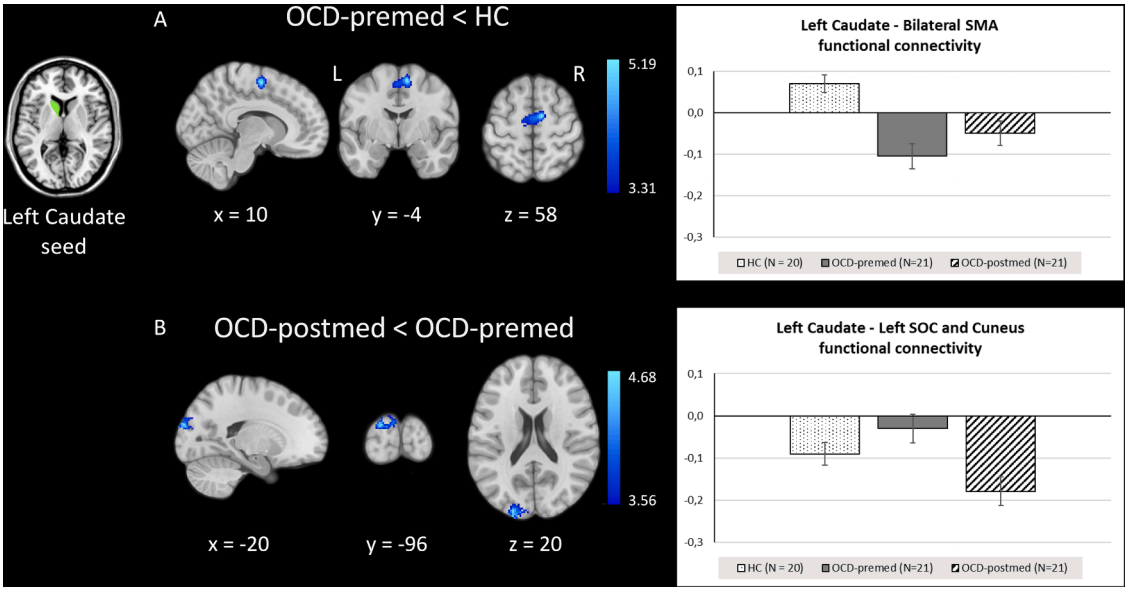


Fig. 4. Functional connectivity differences for the left caudate seed. **A)** Increased anticorrelation with bilateral SMA in OCD-premed compared to HCs. **B)** Increased anticorrelation with left SOC and cuneus in OCD-postmed compared to OCD-premed (cluster forming threshold uncorrected $p < 0.001$, cluster-level $p_{FWE\text{-}corr} < 0.0026$). Bar graphs depicting the correlation values for HC, OCD-premed and OCD-postmed.
SMA: supplementary motor area, SOC: superior occipital cortex, OCD-premed: unmedicated OCD patients, OCD-postmed: OCD patients after treatment, HC: healthy control, L: left, R: right.

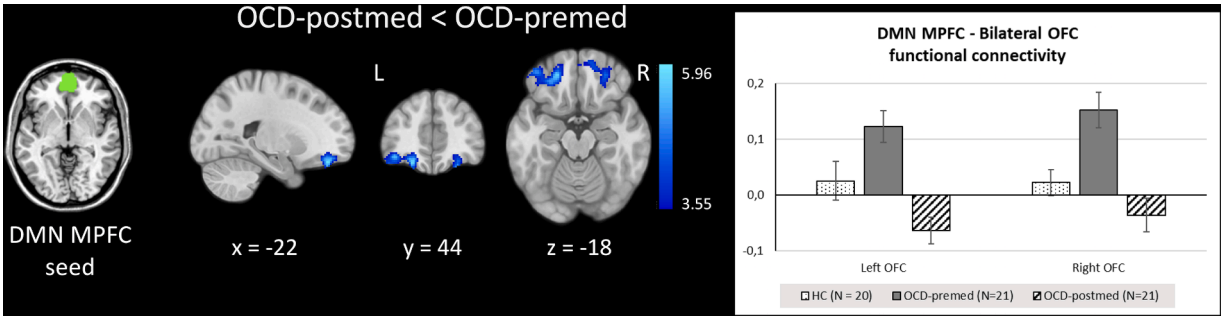


Fig. 5. Functional connectivity differences for the MPFC seed probing the DMN. Hypoconnectivity with two clusters corresponding to the left and right OFC in OCD-postmed compared to OCD-premed (cluster forming threshold uncorrected $p < 0.001$, cluster-level $p_{FWE\text{-}corr} < 0.0026$). Bar graphs depicting the correlation values for HC, OCD-premed and OCD-postmed.
DMN: default mode network, MPFC: medial prefrontal cortex, OFC: orbitofrontal cortex, OCD-premed: unmedicated OCD patients, OCD-postmed: OCD patients after treatment, HC: healthy control, L: left, R: right.

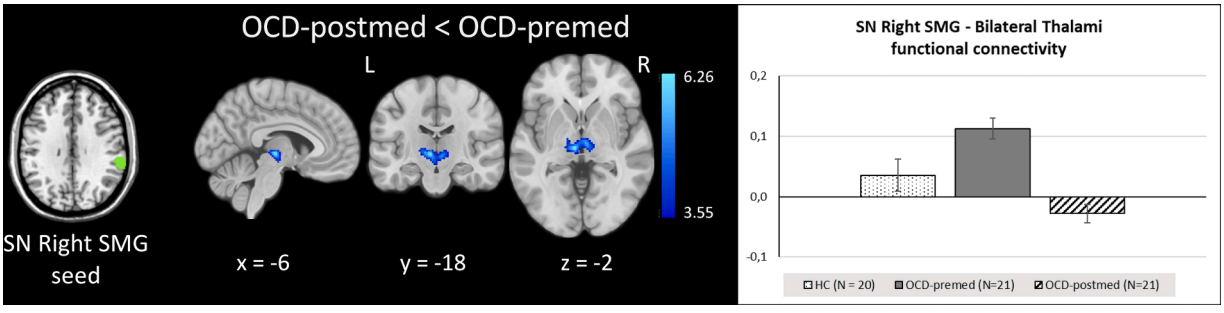


Fig. 6. Functional connectivity differences for the right SMG seed probing the SN. Hypoconnectivity with bilateral thalami in OCD-postmed compared to OCD-premed (cluster forming threshold uncorrected $p < 0.001$, cluster-level $p_{FWE\text{-}corr} < 0.0026$). Bar graphs depicting the correlation values for HC, OCD-premed and OCD-postmed.
SN: salience network, SMG: supramarginal gyrus, OCD-premed: unmedicated OCD patients, OCD-postmed: OCD patients after treatment, HC: healthy control, L: left, R: right.

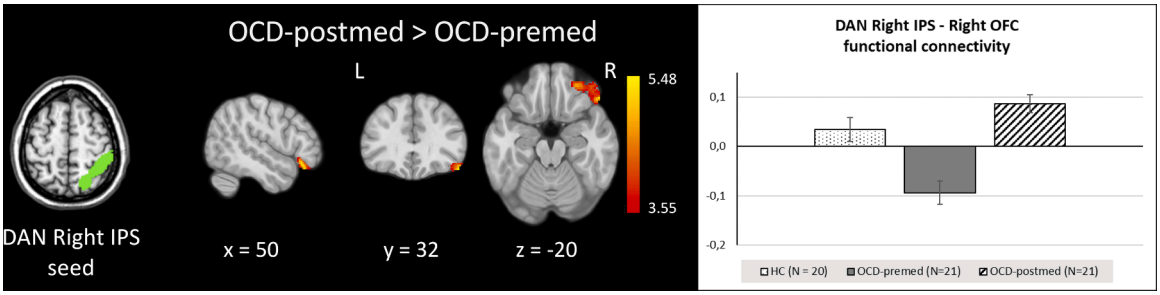


Fig. 7. Functional connectivity differences for the right IPS seed probing the DAN. Hyperconnectivity with right OFC in OCD-postmed compared to OCD-premed (cluster forming threshold uncorrected $p < 0.001$, cluster-level $p_{FWE\text{-}corr} < 0.0026$). Bar graphs depicting the correlation values for HC, OCD-premed and OCD-postmed.
DAN: dorsal attention network, IPS: intraparietal sulcus, OFC: orbitofrontal cortex, OCD-premed: unmedicated OCD patients, OCD-postmed: OCD patients after treatment, HC: healthy control, L: left, R: right.

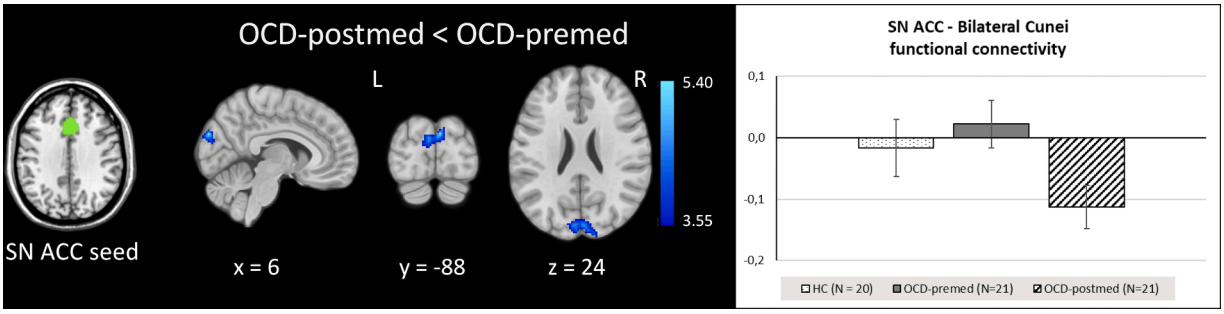


Fig. 8. Functional connectivity differences for the ACC seed probing the SN. Increased anticorrelation with bilateral cunei in OCD-postmed compared to OCD-premed (cluster forming threshold uncorrected $p < 0.001$, cluster-level $p_{FWE\text{-}corr} < 0.0026$). Bar graphs depicting the correlation values for HC, OCD-premed and OCD-postmed.
SN: salience network, ACC: anterior cingulate cortex, OCD-premed: unmedicated OCD patients, OCD-postmed: OCD patients after treatment, HC: healthy control, L: left, R: right.

the treatment introduced a significantly increased anticorrelation with these areas compared with the un-medicated patients ($p_{FWE\text{-}corr}$=0.0005) (Table 4, Fig. 8). The bar graphs in Fig. 8 depicting the mean connectivity values of the ACC seed in HC, unmedicated and medicated OCD patients displays that in this case the medication induced a change, which is also dissimilar to the HC group, even though statistical comparison between the HC and the medicated OCD patients did not support such difference.

3.4. Functional connectivity correlations with the clinical improvement

To test any predictive value of the FC on clinical improvement, we focused on the seed, which displayed a significant difference between the unmedicated patients and HCs and a clear amelioration towards normal values after medication. As left FEF's connectivity with the right IPL was the only finding that fulfills this requirement (Table 3), the baseline FC values of the right IPL areas ($x = 58$, y=−26, $z = 52$) obtained in HC vs unmedicated OCD comparison were tested for correlations with the percent change of the Y-BOCS obsession and compulsion scores due to treatment (Fig. 9). Significant results surviving Bonferroni corrected alpha level of p<0.025 (0.05/2) for the two-tailed correlation with the obsession and compulsion scores of the Y-BOCS revealed that the mean functional connectivity of the ROI was positively correlated with the percentage of the clinical improvement in the Y-BOCS obsession score (Spearman's rho=0.529, $p = 0.014$) (Fig. 9, Table 5).

4. Discussion

With the aim of investigating the intrinsic connectivity alterations at baseline and after treatment in OCD patients, we performed seed to voxel connectivity analyses using bilateral basal ganglia seeds as well as specific seeds of four cognitive networks (DMN, SN, DAN and FPN) previously reported to be affected in OCD (Stern et al., 2012; Chen et al., 2018; Fan et al., 2017; Lee et al., 2020). Compared to the HCs, OCD patients showed increased FC both within the DAN and between the DAN and FPN, whereas an anticorrelation was observed in the motor loop between the left caudate seed and the SMA in the untreated OCD group. Among these baseline findings, anticorrelation observed in the motor loop did not significantly change with treatment, while the within DAN/DAN to FPN hyperconnectivity between the left FEF and right IPL was significantly ameliorated after medication. A similar trend was also present for the left FEF-left IPL connectivity, although the treatment-dependent reduction of this hyperconnectivity did not reach a statistically significant level. These DAN/DAN to FPN connectivity findings that display a consistent effect through both the OCD-premed vs HC and the OCD-premed vs OCD-postmed comparisons also significantly correlated with the clinical improvement in obsession scores.

4.1. Baseline DAN hyperconnectivity ameliorated by medication

Our findings revealed that aberrant DAN intra-network and DAN (left FEF) to FPN (IPL) between-network hyperconnectivities at pre-treatment stage, which were positively correlated with the percentage of the treatment-related clinical improvement in Y-BOCS obsession score, were significantly ameliorated with medication.

Although a majority of studies on OCD mostly focused on the triple network model and so preferred not to investigate the DAN related alterations (Gürsel et al., 2018), some studies point out aberrant intra- and inter-network FCs including DAN in OCD patients (Brennan et al., 2019; Lee et al., 2020). The DAN, with the major nodes of the bilateral FEF and

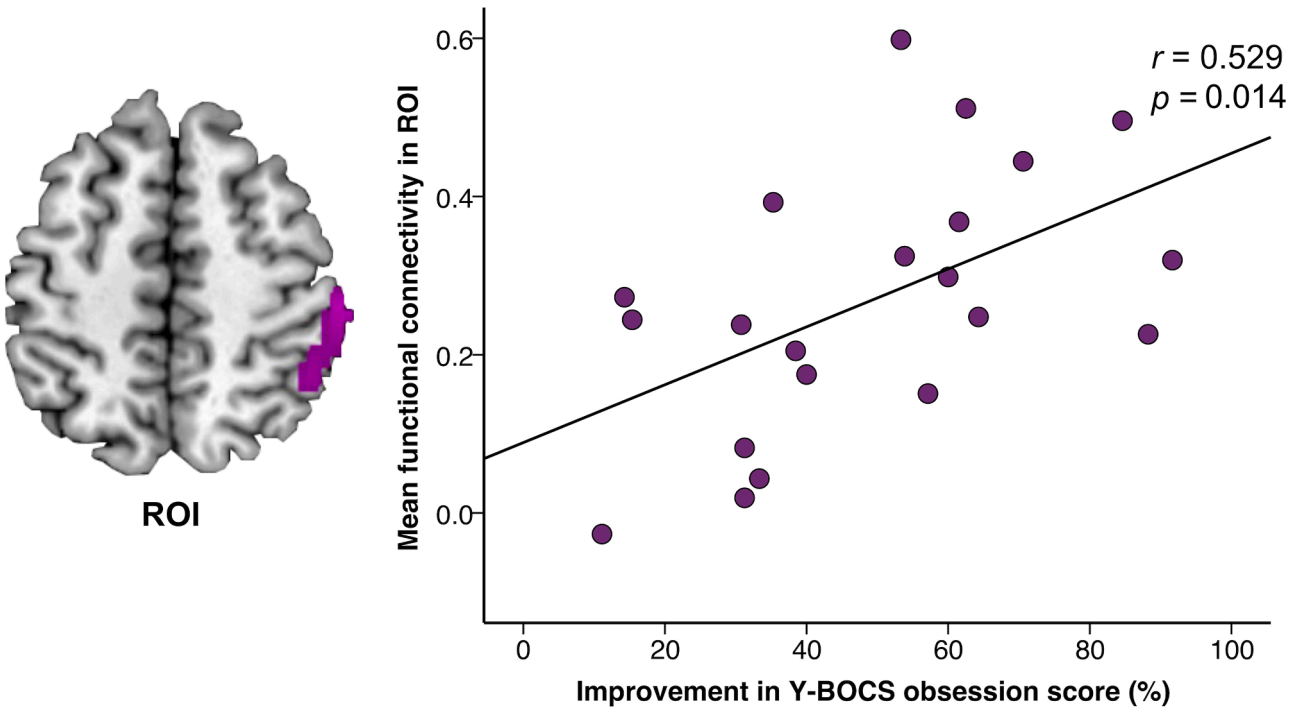


Fig. 9. Spearman's correlation between the clinical improvement in Y-BOCS obsession score and mean functional connectivity in the ROI (right IPL) that showed a significant connectivity difference with the left FEF seed of the DAN between the unmedicated OCD patients and HCs. The scatter plot shows a positive correlation in OCD patients between the percentage of the improvement in Y-BOCS obsession score and mean functional connectivity in this ROI in unmedicated OCD patients (Bonferroni corrected alpha level $p < 0.025$, two-tailed).
Y-BOCS: The Yale–Brown Obsessive-Compulsive Scale, ROI: region of interest, IPL: inferior parietal lobule, FEF: frontal eye field, DAN: dorsal attention network, OCD: obsessive compulsive disorder, HCs: healthy controls.

Table 5
Spearman's correlation between mean value of the left FEF seed of the DAN to right IPL connectivity and the clinical improvement in Y-BOCS scores ($N = 21$).

	ROI	Y-BOCS Obsession	Y-BOCS Compulsion
ROI	$r = 1.00$		
Y-BOCS Obsession	$\mathbf{r = 0.529}$		
	$\mathbf{p = 0.014}$		
Y-BOCS Compulsion	$r = 0.375$	$\mathbf{r = 0.851}$	$r = 1.00$
	$p = 0.094$	$\mathbf{p < 0.001}$	

Y-BOCS: The Yale–Brown Obsessive Compulsive Scale.
Bold indicates significant correlations at alpha level of $p < 0.025$ (0.05/2) Bonferroni corrected (two-tailed).

IPS, is involved in the top-down process of externally oriented actions and perceptions and the source of attentional control signals (Pagliaccio et al., 2021). On the other hand, the FPN is involved in maintaining and manipulating information in working memory as well as rule-based problem solving and decision-making in goal-directed behavior (Menon, 2011; Uddin et al., 2019). A meta-analytic study by Dixon et al. (2018), revealed a flexible and heterogeneous FPN organization that may in part emerge from two separable processing streams based on current cognitive demands: (i) DMN connections that may be preferentially involved in the regulation of introspective processes, and (ii) DAN connections that may be preferentially involved in the regulation of visuospatial perceptual attention. In this context, our finding of the hyperconnectivity between the left FEF of the DAN and bilateral IPLs of the FPN may indicate a dysregulation of visuospatial perceptual attention in unmedicated OCD patients.

IPL, one of the core regions of the FPN (Göttlich et al., 2014), is known to play a role in visuospatial working memory (Xia et al., 2020). Impairments in switching from internal thoughts and recalling information about visual stimuli (Shin et al., 2014a) and visual memory (Kwon et al., 2009) in OCD patients have been previously argued to be related with the IPL dysfunction. IPL is also thought to be responsible for cognitive deficits in attention, planning, and response inhibition in patients with OCD (Menzies et al., 2008; Göttlich et al., 2014). Considering the studies examining FC alterations between the large-scale networks in OCD patients and treatment responses, DAN seems to be crucial for understanding the mechanism underpinning the OCD pathology, in addition to the triple network model. In their study showing altered FC within DAN, Pagliaccio et al. (2021) suggested that higher negative DAN-DMN connectivity is a potential predictor of worsening obsessive-compulsive symptoms in pediatric groups. Another study by Kim et al. (2020) showed a lower inter-network connectivity between these two networks during a planning task, which normalized after 16 weeks of SSRI treatment (Kim et al., 2020). Shin and coworkers (2014) also reported a similar SSRI treatment effect on FC of the large-scale networks including the FPN. It is claimed that OCD symptom severity was best predicted by both within- and cross-network connections involving DAN, which is interpreted as a connectivity biomarker (Brennan et al., 2019). A recent connectome-wide study investigating the relationship between the obsession and rs-FC in OCD patients showed a relation between the obsession severity and the FPN-DAN inter-network connectivity (Lee et al., 2020). In line with the outstanding previous findings of DAN intra- and inter-network connectivity changes in OCD, our study also revealed treatment-related changes in DAN and DAN to FPN connectivity in OCD patients. Given that the increased FC normalized after 12 weeks of escitalopram treatment, it is clear that the aberrant FC observed in the OCD patients responded well to the medication. Most importantly, since the aberrant FC at baseline was correlated with at least one of the two global symptom scores, we suggest this baseline DAN to FPN hyperconnectivity may be a new potential neuroimaging marker to predict the treatment response in OCD patients.

4.2. Anticorrelation between the caudate and SMA normalized with medication

In the present study, untreated OCD patients compared to HCs demonstrated an anticorrelation between the left caudate seed and the SMA. After medication, this abnormal connectivity seems to be normalized as no significant difference is observed in the comparison of the medicated OCD patients with the HC participants. While the absence of a direct effect of the medication on this anticorrelation in terms of a significant difference between the medicated vs unmedicated patients' FC maps weakens the strength of this result, an indirect sign of medication effect can still be claimed for this FC result.

The caudate nucleus, with extensive frontal connections throughout the CSTC circuits (Hou et al., 2014), was considered a critical subcortical region involved in the pathophysiology of OCD. Numerous studies on OCD patients have demonstrated abnormal activity in the caudate nucleus (Kang et al., 2013; Hou et al., 2014; Posner et al., 2014). It is associated with planning the execution of the movement and cognitive functions such as response inhibition, planning and flexibility (Del Casale et al., 2016; Ping et al., 2013). SMA is a cortical region that is associated with complex motor control functions and also closely related to executive functions such as response inhibition, set shifting, rule learning and error monitoring (Nachev et al., 2008; Bonini et al., 2014). Repetitive transcranial magnetic stimulation to the SMA reduces compulsive behaviors (Gomes et al., 2012; Hawken et al., 2016). Such abnormalities in the SMA activation may underlie compulsive behaviors in patients with OCD (Cheng et al., 2013).

A FC study by Chen et al. (2016) showed hyperconnectivity between the left caudate nucleus and right SMA in patients with OCD. Similarly, increased rs-FC among the left caudate, right thalamus and bilateral SMA has been recently reported (Zhang et al., 2021). Authors suggested that this abnormal connection of striatum and SMA may interfere with flexible transition between habitual and goal-directed behaviors, resulting in stereotyped and/or compulsive behavior in OCD. Altered activation in the striatum may be linked to excitatory projections from the SMA (Mantovani et al., 2021). Moreover, a recent study (Lee et al., 2020) showing that obsession severity is correlated with multivariate patterns of connectivity in the SMA, suggested that sensory-motor integration through SMA-centered circuits may play a key role in causing obsessions with insufficient inhibition or overabundance of intrusive and repetitive thoughts that internally triggered in OCD patients. A recent meta-analysis of resting-state fMRI data by ENIGMA-OCD Consortium also highlights the sensorimotor network aberration in OCD (Bruin et al., 2023).

The majority of the patients recruited in the previous studies by Chen et al. (2016) and Zhang et al. (2021) were under medication (SSRIs and/or SNRIs, even antipsychotics). This may explain the discrepancy between the inter-network hyper-connectivity findings of the caudate nucleus and SMA reported in the aforementioned studies and the anticorrelation we found, which subsequently normalized with the treatment. On the other hand, this hyperconnectivity between the caudate and SMA may also reflect a long-term effect of medication. Since our patient group consisted of unmedicated patients (9 were medication-naïve) with no comorbidity, our research could be considered more reliable and powerful in detecting OCD-specific functional connectivity alterations. These results point out that the abnormal resting-state functional connectivity between the SMA and caudate may be a key characteristic in OCD.

4.3. Treatment related functional connectivity changes

In addition to the straightforward normalizing effect of the treatment on the DAN and FPN and the absence of any clear effect of the treatment on the motor loop hypoconnectivity in the unmedicated OCD patients, additional treatment effects were observed for the left caudate and specific seeds of the DMN, SN and DAN, when the unmedicated and medicated OCD patients were compared. Although such effects initially suggest possible adverse effects of the treatment on FC, considering the role of the between-group variance on the statistical power of the comparisons between the OCD and HC groups in contrast to within-group comparisons between the medicated vs unmedicated OCD patients, we cannot directly suggest that these are medication effects independent of OCD. Indeed, a closer observation of the change of mean z-transformed correlation coefficients of these areas among the HC, unmedicated and medicated patients (Figs. 5-7) points rather to a set of treatment effects that convert the relatively slight connectivity changes in the unmedicated OCD patients towards healthy values. A similar study design on a larger patient group might provide conclusive results on whether these DMN, SN and DAN-related FC changes depend on ameliorating or adverse effects of the treatment.

4.4. Limitations and strenghts

The sample size of the study was not large enough to examine the neuroimaging findings associated with symptom dimensions. Despite this limitation, the recruitment of unmedicated patients (9 were medication-naive) without any comorbidity is a strength of the present study, as this allowed us to detect the OCD-specific neural connectivity changes.

5. Conclusion

Our study showed that baseline DAN to FPN hyperconnectivity may have a potential for being a neuroimaging marker to predict the treatment response in patients with OCD. While our findings support aberrant orchestration within the triple network as previously suggested, it also extends them by showing FC abnormalities in the DAN to FPN, which may help to build a new model on the network dynamics in OCD.

Declaration of Interest Statement

This manuscript has not been published and is not under consideration for publication elsewhere. Hasan Bakay, Cigdem Ulasoglu-Yildiz, Elif Kurt, Tamer Demiralp and Raşit Tükel report no disclosures. We did not receive any specific grant from funding agencies in the public, commercial, or not-for-profit sectors. A written informed consent form was obtained from all participants.

Funding

This study was supported by Istanbul University Scientific Research Projects Unit (Project Number: 20349).

Data availability statement

Data that support the findings are available from the corresponding author on reasonable demand.

CRediT authorship contribution statement

Hasan Bakay: Conceptualization, Methodology, Formal analysis, Data curation, Investigation, Writing – original draft. **Cigdem Ulasoglu-Yildiz:** Conceptualization, Methodology, Validation, Formal analysis, Data curation, Investigation, Writing – original draft, Visualization. **Elif Kurt:** Conceptualization, Methodology, Validation, Formal analysis, Writing – original draft, Visualization. **Tamer Demiralp:** Conceptualization, Methodology, Resources, Writing – review & editing, Visualization, Supervision, Project administration. **Raşit Tükel:** Conceptualization, Methodology, Writing – review & editing, Supervision, Project administration.

Declaration of Competing Interest

The authors declare that they have no conflict of interest.

Acknowledgments

We thank all the participants for their contributions.

References

Abramowitz, J.S., Taylor, S., McKay, D., 2009. Obsessive-compulsive disorder. Lancet 374 (9688), 491–499. https://doi.org/10.1016/S0140-6736(09)60240-3.

Beucke, J.C., Sepulcre, J., Talukdar, T., Linnman, C., Zschenderlein, K., Endrass, T., Kaufmann, C., Kathmann, N., 2013. Abnormally high degree connectivity of the orbitofrontal cortex in obsessive-compulsive disorder. JAMA Psychiatry 70 (6), 619–629. https://doi.org/10.1001/jamapsychiatry.2013.173.

Bonini, F., Burle, B., Liégeois-Chauvel, C., Régis, J., Chauvel, P., Vidal, F., 2014. Action monitoring and medial frontal cortex: leading role of supplementary motor area. Science 343 (6173), 888–891. https://doi.org/10.1126/science.1247412.

Brennan, B.P., Wang, D., Li, M., Perriello, C., Ren, J., Elias, J.A., Van Kirk, N.P., Krompinger, J.W., Pope Jr, H.G., Haber, S.N., et al., 2019. Use of an individual-level approach to identify cortical connectivity biomarkers in obsessive-compulsive disorder. biological psychiatry. Cognit. Neurosci. Neuroimag. 4 (1), 27–38. https://doi.org/10.1016/j.bpsc.2018.07.014.

Bruin, W.B., Abe, Y., Alonso, P., Anticevic, A., Backhausen, L.L., Balachander, S., van Wingen, G.A., 2023. The functional connectome in obsessive-compulsive disorder: resting-state mega-analysis and machine learning classification for the ENIGMA-OCD consortium. Mol. Psychiatry. https://doi.org/10.1038/s41380-023-02077-0, 10.1038/s41380-023-02077-0.

Chai, X.J., Castañón, A.N., Ongür, D., Whitfield-Gabrieli, S., 2012. Anticorrelations in resting state networks without global signal regression. Neuroimage 59 (2), 1420–1428. https://doi.org/10.1016/j.neuroimage.2011.08.048.

Chen, Y.H., Li, S.F., Lv, D., Zhu, G.D., Wang, Y.H., Meng, X., Hu, Q., Li, C.C., Zhang, L.T., Chu, X.P., et al., 2018. Decreased intrinsic functional connectivity of the salience network in drug-naïve patients with obsessive-compulsive disorder. Front. Neurosci. 12, 889. https://doi.org/10.3389/fnins.2018.00889.

Chen, Y., Juhás, M., Greenshaw, A.J., Hu, Q., Meng, X., Cui, H., Ding, Y., Kang, L., Zhang, Y., Wang, Y., et al., 2016. Abnormal resting-state functional connectivity of the left caudate nucleus in obsessive-compulsive disorder. Neurosci. Lett. 623, 57–62. https://doi.org/10.1016/j.neulet.2016.04.030.

Cheng, Y., Xu, J., Nie, B., Luo, C., Yang, T., Li, H., Lu, J., Xu, L., Shan, B., Xu, X., 2013. Abnormal resting-state activities and functional connectivities of the anterior and the posterior cortexes in medication-naïve patients with obsessive-compulsive disorder. PLoS One 8 (6), e67478. https://doi.org/10.1371/journal.pone.0067478.

Cui, G., Ou, Y., Chen, Y., Lv, D., Jia, C., Zhong, Z., Yang, R., Wang, Y., Meng, X., Cui, H., et al., 2020. Altered global brain functional connectivity in drug-naive patients with obsessive-compulsive disorder. Front. Psychiatry 11, 98. https://doi.org/10.3389/fpsyt.2020.00098.

Del Casale, A., Rapinesi, C., Kotzalidis, G.D., De Rossi, P., Curto, M., Janiri, D., Criscuolo, S., Alessi, M.C., Ferri, V.R., De Giorgi, R., et al., 2016. Executive functions in obsessive-compulsive disorder: an activation likelihood estimate meta-analysis of fMRI studies. World J. Biol. Psychiatry 17 (5), 378–393. https://doi.org/10.3109/15622975.2015.1102323.

Dixon, M.L., De La Vega, A., Mills, C., Andrews-Hanna, J., Spreng, R.N., Cole, M.W., Christoff, K, 2018. Heterogeneity within the frontoparietal control network and its relationship to the default and dorsal attention networks. Proc. Natl. Acad. Sci. U.S.A. 115 (7), E1598–E1607. https://doi.org/10.1073/pnas.1715766115.

Fan, J., Zhong, M., Gan, J., Liu, W., Niu, C., Liao, H., Zhang, H., Yi, J., Chan, R., Tan, C., et al., 2017. Altered connectivity within and between the default mode, central executive, and salience networks in obsessive-compulsive disorder. J. Affect. Disord. 223, 106–114. https://doi.org/10.1016/j.jad.2017.07.041.

Gomes, P.V., Brasil-Neto, J.P., Allam, N., Rodrigues de Souza, E., 2012. A randomized, double-blind trial of repetitive transcranial magnetic stimulation in obsessive-compulsive disorder with three-month follow-up. J. Neuropsychiatry Clin. Neurosci. 24 (4), 437–443. https://doi.org/10.1176/appi.neuropsych.11100242.

Göttlich, M., Krämer, U.M., Kordon, A., Hohagen, F., Zurowski, B., 2014. Decreased limbic and increased fronto-parietal connectivity in unmedicated patients with obsessive-compulsive disorder. Hum. Brain Mapp. 35 (11), 5617–5632. https://doi.org/10.1002/hbm.22574.

Gürsel, D.A., Avram, M., Sorg, C., Brandl, F., Koch, K., 2018. Frontoparietal areas link impairments of large-scale intrinsic brain networks with aberrant fronto-striatal interactions in OCD: a meta-analysis of resting-state functional connectivity. Neurosci. Biobehav. Rev. 87, 151–160. https://doi.org/10.1016/j.neubiorev.2018.01.016.

Gürsel, D.A., Reinholz, L., Bremer, B., Schmitz-Koep, B., Franzmeier, N., Avram, M., Koch, K., 2020. Frontoparietal and salience network alterations in obsessive–compulsive disorder: insights from independent component and sliding time window analyses. J. Psychiatry 45 (3), 214–221. https://doi.org/10.1503/jpn.190038.

Hawken, E.R., Dilkov, D., Kaludiev, E., Simek, S., Zhang, F., Milev, R., 2016. Transcranial magnetic stimulation of the supplementary motor area in the treatment of obsessive-compulsive disorder: a multi-site study. Int. J. Mol. Sci. 17 (3), 420. https://doi.org/10.3390/ijms17030420.

Hou, J.M., Zhao, M., Zhang, W., Song, L.H., Wu, W.J., Wang, J., Zhou, D.Q., Xie, B., He, M., Guo, J.W., et al., 2014. Resting-state functional connectivity abnormalities in patients with obsessive-compulsive disorder and their healthy first-degree relatives. J Psychiatry 39 (5), 304–311. https://doi.org/10.1503/jpn.130220.

Hou, J., Wu, W., Lin, Y., Wang, J., Zhou, D., Guo, J., Gu, S., He, M., Ahmed, S., Hu, J., et al., 2012. Localization of cerebral functional deficits in patients with obsessive-compulsive disorder: a resting-state fMRI study. J. Affect. Disord. 138 (3), 313–321. https://doi.org/10.1016/j.jad.2012.01.022.

Kang, D.H., Jang, J.H., Han, J.Y., Kim, J.H., Jung, W.H., Choi, J.S., Choi, C.H., Kwon, J. S., 2013. Neural correlates of altered response inhibition and dysfunctional connectivity at rest in obsessive-compulsive disorder. Prog. Neuropsychopharmacol. Biol. Psychiatry 40, 340–346. https://doi.org/10.1016/j.pnpbp.2012.11.001.

Kim, M., Jung, W.H., Shim, G., Kwon, J.S., 2020. The effects of selective serotonin reuptake inhibitors on brain functional networks during goal-directed planning in obsessive-compulsive disorder. Sci. Rep. 10 (1), 20619. https://doi.org/10.1038/s41598-020-77814-4.

Kwon, J.S., Jang, J.H., Choi, J.S., Kang, D.H., 2009. Neuroimaging in obsessive-compulsive disorder. Expert. Rev. Neurother. 9 (2), 255–269. https://doi.org/10.1586/14737175.9.2.255.

Lee, T.Y., Jung, W.H., Kwak, Y.B., Yoon, Y.B., Lee, J., Kim, M., Kim, E., Kwon, J.S., 2020. Distinct neural networks associated with obsession and delusion: a connectome-wide association study. Psychol. Med. 1–9. https://doi.org/10.1017/S0033291720000057. Advance online publication.

Li, P., Yang, X., Greenshaw, A.J., Li, S., Luo, J., Han, H., Liu, J., Zhong, Z., Guo, Z., Xiong, H., et al., 2018. The effects of cognitive behavioral therapy on resting-state functional brain network in drug-naive patients with obsessive-compulsive disorder. Brain Behav. 8 (5), e00963. https://doi.org/10.1002/brb3.963.

Mantovani, A., Neri, F., D'Urso, G., Mencarelli, L., Tatti, E., Momi, D., Menardi, A., Sprugnoli, G., Santarnecchi, E., Rossi, S., 2021. Functional connectivity changes and symptoms improvement after personalized, double-daily dosing, repetitive transcranial magnetic stimulation in obsessive-compulsive disorder: a pilot study. J. Psychiatr. Res. 136, 560–570. https://doi.org/10.1016/j.jpsychires.2020.10.030.

Menon, V., 2011. Large-scale brain networks and psychopathology: a unifying triple network model. Trends Cogn. Sci. (Regul. Ed.) 15 (10), 483–506. https://doi.org/10.1016/j.tics.2011.08.003.

Menzies, L., Chamberlain, S.R., Laird, A.R., Thelen, S.M., Sahakian, B.J., Bullmore, E.T., 2008. Integrating evidence from neuroimaging and neuropsychological studies of obsessive-compulsive disorder: the orbitofronto-striatal model revisited. Neurosci. Biobehav. Rev. 32 (3), 525–549. https://doi.org/10.1016/j.neubiorev.2007.09.005.

Nachev, P., Kennard, C., Husain, M., 2008. Functional role of the supplementary and pre-supplementary motor areas. Nat. Rev. Neurosci. 9 (11), 856–869. https://doi.org/10.1038/nrn2478.

Nieto-Castanon, A., 2020. Handbook of Functional Connectivity Magnetic Resonance Imaging Methods in CONN. Hilbert Press, Boston, MA. https://doi.org/10.56441/hilbertpress.2207.6598.

Nieto-Castanon, A. & Whitfield-Gabrieli, S. (2020). CONN functional connectivity toolbox: RRID SCR_009550, release 20. doi:10.56441/hilbertpress.2048.3738.

Pagliaccio, D., Durham, K., Fitzgerald, K.D., Marsh, R., 2021. Obsessive-compulsive symptoms among children in the adolescent brain and cognitive development study: clinical, cognitive, and brain connectivity correlates. biological psychiatry. Cognit. Neurosci. Neuroimag. 6 (4), 399–409. https://doi.org/10.1016/j.bpsc.2020.10.019.

Ping, L., Su-Fang, L., Hai-Ying, H., Zhang-Ye, D., Jia, L., Zhi-Hua, G., Hong-Fang, X., Yu-Feng, Z., Zhan-Jiang, L., 2013. Abnormal spontaneous neural activity in obsessive-compulsive disorder: a resting-state functional magnetic resonance imaging study. PLoS One 8 (6), e67262. https://doi.org/10.1371/journal.pone.0067262.

Posner, J., Marsh, R., Maia, T.V., Peterson, B.S., Gruber, A., Simpson, H.B., 2014. Reduced functional connectivity within the limbic cortico-striato-thalamo-cortical loop in unmedicated adults with obsessive-compulsive disorder. Hum. Brain Mapp. 35 (6), 2852–2860. https://doi.org/10.1002/hbm.22371.

Reggente, N., Moody, T.D., Morfini, F., Sheen, C., Rissman, J., O'Neill, J., Feusner, J.D., 2018. Multivariate resting-state functional connectivity predicts response to cognitive behavioral therapy in obsessive-compulsive disorder. Proc. Natl. Acad. Sci. U.S.A. 115 (9), 2222–2227. https://doi.org/10.1073/pnas.1716686115.

Saxena, S., Brody, A.L., Schwartz, J.M., Baxter, L.R., 1998. Neuroimaging and frontal-subcortical circuitry in obsessive-compulsive disorder. Br. J. Psychiatry Suppl. (35), 26–37.

Shin, D.J., Jung, W.H., He, Y., Wang, J., Shim, G., Byun, M.S., Jang, J.H., Kim, S.N., Lee, T.Y., Park, H.Y., Kwon, J.S., 2014a. The effects of pharmacological treatment on functional brain connectome in obsessive-compulsive disorder. Biol. Psychiatry 75 (8), 606–614. https://doi.org/10.1016/j.biopsych.2013.09.002.

Shin, N.Y., Lee, T.Y., Kim, E., Kwon, J.S., 2014b. Cognitive functioning in obsessive-compulsive disorder: a meta-analysis. Psychol. Med. 44 (6), 1121–1130. https://doi.org/10.1017/S0033291713001803.

Stern, E.R., Fitzgerald, K.D., Welsh, R.C., Abelson, J.L., Taylor, S.F., 2012. Resting-state functional connectivity between fronto-parietal and default mode networks in obsessive-compulsive disorder. PLoS One 7 (5), e36356. https://doi.org/10.1371/journal.pone.0036356.

Tian, L., Meng, C., Jiang, Y., Tang, Q., Wang, S., Xie, X., Fu, X., Jin, C., Zhang, F., Wang, J., 2016. Abnormal functional connectivity of brain network hubs associated with symptom severity in treatment-naive patients with obsessive-compulsive disorder: a resting-state functional MRI study. Prog. Neuropsychopharmacol. Biol. Psychiatry 66, 104–111. https://doi.org/10.1016/j.pnpbp.2015.12.003.

Uddin, L.Q., Yeo, B., Spreng, R.N., 2019. Towards a universal taxonomy of macro-scale functional human brain networks. Brain Topogr. 32 (6), 926–942. https://doi.org/10.1007/s10548-019-00744-6.

Xia, J., Fan, J., Liu, W., Du, H., Zhu, J., Yi, J., Tan, C., Zhu, X., 2020. Functional connectivity within the salience network differentiates autogenous- from reactive-type obsessive-compulsive disorder. Prog. Neuropsychopharmacol. Biol. Psychiatry 98, 109813. https://doi.org/10.1016/j.pnpbp.2019.109813.

Xu, T., Zhao, Q., Wang, P., Fan, Q., Chen, J., Zhang, H., Yang, Z., Stein, D.J., Wang, Z., 2019. Altered resting-state cerebellar-cerebral functional connectivity in obsessive-compulsive disorder. Psychol. Med. 49 (7), 1156–1165. https://doi.org/10.1017/S0033291718001915.

Yang, X.Y., Sun, J., Luo, J., Zhong, Z.X., Li, P., Yao, S.M., Xiong, H.F., Huang, F.F., Li, Z. J., 2015. Regional homogeneity of spontaneous brain activity in adult patients with obsessive-compulsive disorder before and after cognitive behavioural therapy. J. Affect. Disord. 188, 243–251. https://doi.org/10.1016/j.jad.2015.07.048.

Yang, X., Hu, X., Tang, W., Li, B., Yang, Y., Gong, Q., Huang, X., 2019. Multivariate classification of drug-naive obsessive-compulsive disorder patients and healthy controls by applying an SVM to resting-state functional MRI data. BMC Psychiatry 19 (1), 210. https://doi.org/10.1186/s12888-019-2184-6.

Zhang, Y., Liao, J., Li, Q., Zhang, X., Liu, L., Yan, J., Zhang, D., Yan, H., Yue, W., 2021. Altered resting-state brain activity in schizophrenia and obsessive-compulsive disorder compared with non-psychiatric controls: commonalities and distinctions across disorders. Front. Psychiatry 12, 681701. https://doi.org/10.3389/fpsyt.2021.681701.